CONTROLLED SYNTHESIS, SPECTRAL STUDIES, AND CATALYTIC ACTIVITY OF SILVER AND GOLD NANOPARTICLES BIOSYNTHESIZED USING *Ficus sycomorus* LEAF EXTRACT**

M. F. Zayed [1*], O. M. Shalby [1], W. H. Eisa [2], S. M. El-Kousy [1], A. M. Eltorgoman [1]

[1] Chemistry Department, Faculty of Science, Menoufia University, Egypt; e-mail: mervat.zayed@yahoo.com
[2] Spectroscopy Department, Physics Division, National Research Centre (NRC), Egypt

Plant-mediated synthesis of nanoparticles (NPs) is an efficient and safe alternative to the conventional synthetic route. In this study, silver and gold NPs (AgNPs and AuNPs, respectively) were synthesized via a green route using Ficus sycomorus extract. Tuning the experimental parameters (namely, extract quantity, metal ion concentration, and pH value) allowed control over the size, shape, and size distribution of the NPs. UV-visible spectroscopy has been utilized to monitor the spectral profile changes of the surface plasmon resonance of the NPs under various conditions. The successful preparation of monodispersed spherical AgNPs (4 nm) and AuNPs (11 nm) was confirmed by transmission electron microscopic analysis. Fourier transform infrared spectroscopic data indicated that flavonoid glycosides played a major role in the reduction and stabilization of metal ions. The as-prepared AgNPs and AuNPs were then used as green catalysts for efficient degradation of methylene blue in the presence of sodium borohydride.

Keywords: *Ficus sycomorus, gold nanoparticles, silver nanoparticles, controlled synthesis, catalytic activity.*

КОНТРОЛИРУЕМЫЙ СИНТЕЗ, СПЕКТРАЛЬНЫЕ ИССЛЕДОВАНИЯ И КАТАЛИТИЧЕСКАЯ АКТИВНОСТЬ НАНОЧАСТИЦ СЕРЕБРА И ЗОЛОТА, СИНТЕЗИРОВАННЫХ С ИСПОЛЬЗОВАНИЕМ ЭКСТРАКТА ЛИСТЬЕВ *Ficus sycomorus*

M. F. Zayed [1*], O. M. Shalby [1], W. H. Eisa [2], S. M. El-Kousy [1], A. M. Eltorgoman [1]

УДК 543.42;620.3;66.097.3

[1] Университет Менуфия, Эль-Менуфия, Египет; e-mail: mervat.zayed@yahoo.com
[2] Национальный исследовательский центр (NRC), Египет

(Поступила 9 марта 2021)

Наночастицы серебра (AgNPs) и золота (AuNPs) синтезированы экологически чистым методом с использованием экстракта Ficus sycomorus. Настройка экспериментальных параметров (количества извлеченного, концентрации ионов металлов и значения pH) позволяет контролировать размер, форму и распределение наночастиц по размерам. С помощью УФ-видимой спектроскопии выявлены изменения спектрального профиля поверхностного плазмонного резонанса наночастиц в различных условиях. Получение монодисперсных сферических AgNPs (4 нм) и AuNPs (11 нм) подтверждено методом просвечивающей электронной микроскопии. По данным ИК-Фурье-спектроскопии, флавоноидные гликозиды играют главную роль в восстановлении и стабилизации ионов металлов. Свежеприготовленные AgNP и AuNP использованы в качестве экологичных катализаторов для эффективного разложения метиленового синего в присутствии боргидрида натрия.

Ключевые слова: *экстракт Ficus sycomorus, наночастицы золота, наночастицы серебра, контролируемый синтез, каталитическая активность.*

**Full text is published in JAS V. 89, No. 1 (http://springer.com/journal/10812) and in electronic version of ZhPS V. 89, No. 1 (http://www.elibrary.ru/title_about.asp?id=7318; sales@elibrary.ru).

Introduction. AgNPs and AuNPs are the most commonly used metal NPs in many areas such as sensing, catalysis, electronics, agriculture, optics, and biomedicine [1]. The physicochemical properties of the NPs are fundamentally important for adapting their function in nanotechnology. Therefore, research work is now focused on the preparation of NPs with well-defined morphologies, controlled dispersities, and suitable sizes to assess their features for various applications [2]. Controlled fabrication of metal NPs can be achieved by varying the operational parameters, such as reactant concentrations, pH value of the reaction medium, and reaction time [3–6]. Preparation of metal NPs using plants [7–10] is one of the most considered green methods because it is simple, fast, cheap, and suitable for economic production. Furthermore, plant-produced NPs are more stable and more varied in shape and size compared with those formed by microorganisms [11]. However, the mechanism of reduction of metal ions by plants and stabilization of such NPs have not been completely elucidated. Previous reports have revealed that the biosynthesized metal NPs exhibited much better catalytic activity compared with those synthesized chemically [12]. Moreover, the surface functionalities of such biosynthesized NPs affect their catalytic action.

F. sycomorus (known as Sycamore fig) is a semi-deciduous spreading savannah tree belonging to the family Moraceae. In African traditional medicine, *F. sycomorus* is used for the treatment of snake bites, dysentery, diarrhea, jaundice, cold, cough, throat infections, diabetes, inflammation, and mental illness [13, 14]. Previous studies reported that *F. sycomorus* showed antibacterial, antiepileptic, and anticonvulsant activities [15]. The alcoholic extract of the leaves showed high antioxidant activity due to the presence of a considerable amount of phenolic compounds [16]. This prompted us to investigate the ability of *F. sycomorus* leaf extract to reduce Ag^{+} and Au^{3+} ions to their respective NPs.

We introduce a cheap, simple, and green synthetic route for the production of well-defined uniform AgNPs and AuNPs using the renewable *F. sycomorus* leaf extract at ambient temperature. The effect of varying the reaction parameters on the NPs properties was studied in detail. Finally, the catalytic potential of the as-prepared *F. sycomorus*-coated NPs was tested for the reduction of methylene blue (MB) (Scheme 1).

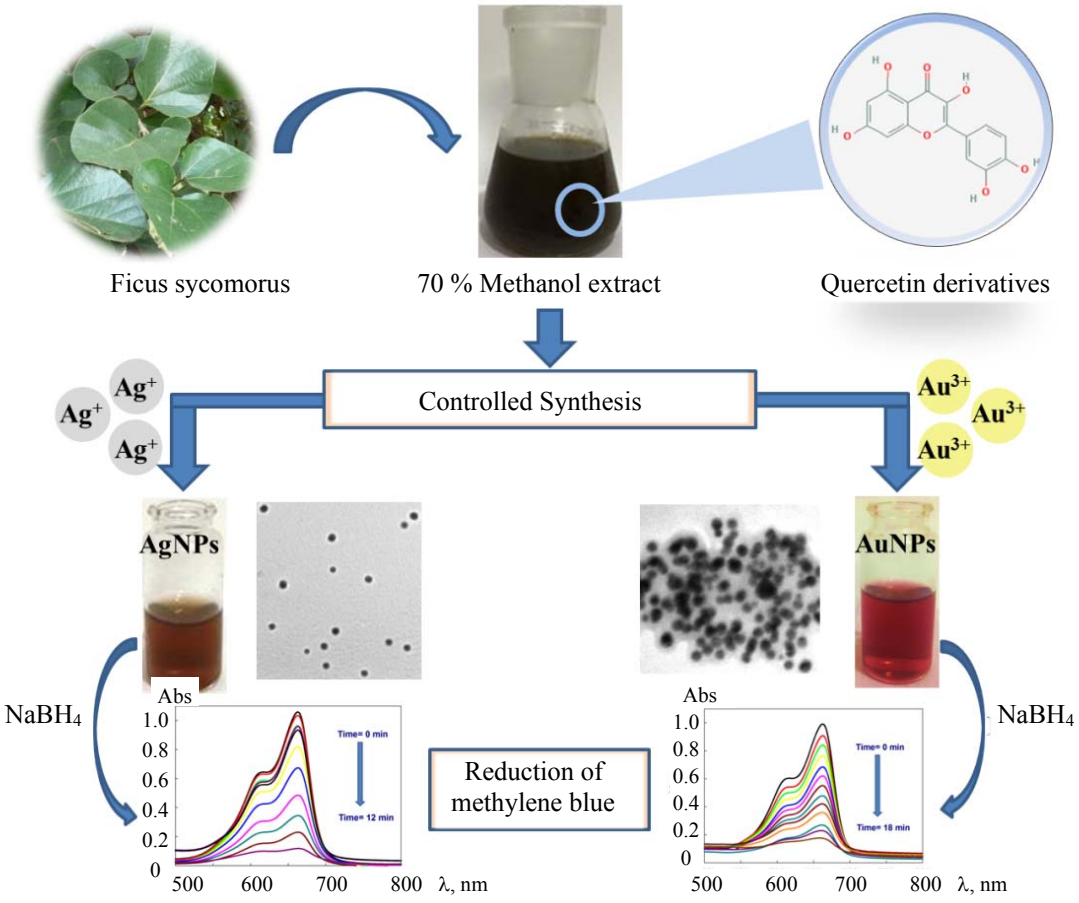

Scheme 1. Biosynthesis of AgNPs and AuNPs for catalytic degradation of MB.

Materials and methods. *F. sycomorus* leaves were collected from Tanta, El-Gharbia, Egypt. Silver nitrate ($AgNO_3$), MB and sodium borohydride ($NaBH_4$) were purchased from Sigma-Aldrich. Tetrachloroauric acid trihydrate ($HAuCl_4 \cdot 3H_2O$) was obtained from Electron Microscopy Sciences.

Preparation of F. sycomorus extract. Fresh *F. sycomorus* leaves (50 g) were washed thoroughly with distilled water then grounded in a blender with a 70% methanol solution (250 mL). The plant material was macerated in the solvent for seven days at room temperature and then filtered through filter paper (Whatman No. 1). The filtrate was stored at −4°C until use.

Biosynthesis of AgNPs and AuNPs. The metal NPs were synthesized using the 70% methanolic *F. sycomorus* leaf extract, which acted as a reducing and capping agent. The preparation method was carried out by adding the plant extract to the metal ion solution ($AgNO_3$ or $HAuCl_4 \cdot 3H_2O$) with stirring at room temperature, then kept in the dark. To remove the unreacted materials, the colloidal suspensions of the NPs were washed repeatedly with 70% aqueous methanol and centrifuged at 8000 rpm for 20 min.

To evaluate the effect of the extract quantities on the NPs synthesis, different quantities (10–100 μL) were used per 5 mL of the metal ion solution (1 mM for $AgNO_3$, 0.5 mM for $HAuCl_4 \cdot 3H_2O$). Experiments were also carried out by varying the metal ion concentration from 0.1 to 1 mM while keeping the extract quantity at 100 μL. The pH value of the reaction varied from 1 to 11. Aqueous solutions of HNO_3 (0.2 M) or NaOH (0.2 M) were used to adjust the pH values of Ag^+ and Au^{3+} solutions.

Catalytic activity of F. sycomorus stabilized NPs in reductive degradation of MB. AgNPs and AuNPs biosynthesized under optimal conditions were tested for their catalytic activity by monitoring the reduction of MB using $NaBH_4$. A typical catalytic reaction was carried out by mixing 25 μL MB stock solution (1 mg/mL) with 2.77 mL deionized water and 50 μL $NaBH_4$ (0.1 M). Then, 50 μL AgNPs or AuNPs was added to the above solution. The degradation process of MB was followed by recording the UV-Vis spectra of the reaction mixture every 1.5 min.

Characterization of F. sycomorus stabilized AgNPs and AuNPs. A UV-Vis spectrophotometer (V-630, Jasco, Japan) was used to monitor both the formation and catalytic activity of the prepared NPs. The shape and sizes of AgNPs and AuNPs were studied by transmission electron microscopy (TEM; JEOL-JEM-1011). Fourier transform-infrared measurements (FTIR) were recorded by a JASCO-6100 spectrometer.

Results and discussion. *Effect of extract quantity on biosynthesis of AgNPs and AuNPs.* The formation of metal NPs can be observed through the color change of the reaction medium. The introduction of *F. sycomorus* extract to $AgNO_3$ and $HAuCl_4$ solutions caused a color change from colorless to brown and from pale yellow to pink, respectively. This color change indicated the formation of AgNPs and AuNPs [17, 18], which was further confirmed by UV-Vis spectroscopy. AgNPs and AuNPs exhibit characteristic surface plasmon resonance (SPR) bands in the UV-spectrum near 400 and 500 nm, respectively, due to the oscillations of free conduction electrons [19, 20]. The intensity, position, and shape of SPR bands are considered as a guide for the size and shape variations of the metal NPs [21]. Hence, the UV-Vis spectrometer is useful for tracking structural attributes caused by changes in the reaction environment.

Figures 1a and b display the UV-Vis spectra of AgNPs and AuNPs biosynthesized using different quantities of *F. sycomorus* extract. For the metal ion solutions with 10 μL/5 mL, weak SPR peaks were observed at 450 and 547 nm for AgNPs and AuNPs, respectively. This indicated the formation of small amounts of metal NPs. The intensity of AgNPs and AuNPs absorption peaks increased as the extract quantity was increased. This may be due to an increase in the active sites necessary for the reduction process, leading to an increase in the NPs production [11]. It was also observed that increasing the extract quantity shifted the SPR bands to shorter wavelengths. This means that smaller NPs were formed at high *F. sycomorus* quantities. The sharpness of the absorption peak relied on the quantity of leaf extract, being sharper at high extract quantities and implying a narrow particle size distribution. The aforementioned results are consistent with the previous studies [6, 22]. The TEM images of AgNPs samples prepared with extract quantities of 25 and 100 μL are presented in Figs. 1c and d. The prepared AgNPs were semi-spherical in shape, and some aggregations/agglomerations of the particles were observed in the two samples. Gaussian curve fitting of the histogram of AgNPs samples indicated that the particle size distribution of AgNPs narrowed with increasing extract quantity. The mean particle size decreased from 14 to 10 nm as the extract quantity increased from 25 to 100 μL, which agrees with the UV-Vis results. The TEM images of AuNPs samples prepared with 25 and 100 μL extract are presented in Figs. 1e and f. Most of the AuNPs prepared with 25 μL extract (Fig. 1e) were highly aggregated/agglomerated and spherical along with a few triangular plates. The size of the spherical AuNPs ranged from 10 to 40 nm, whereas the sizes of the triangular AuNPs were in the range of 40 to 83 nm. As the extract content increased to 100 μL (Fig. 1f), spherical AuNPs with no anisotropic morpholo-

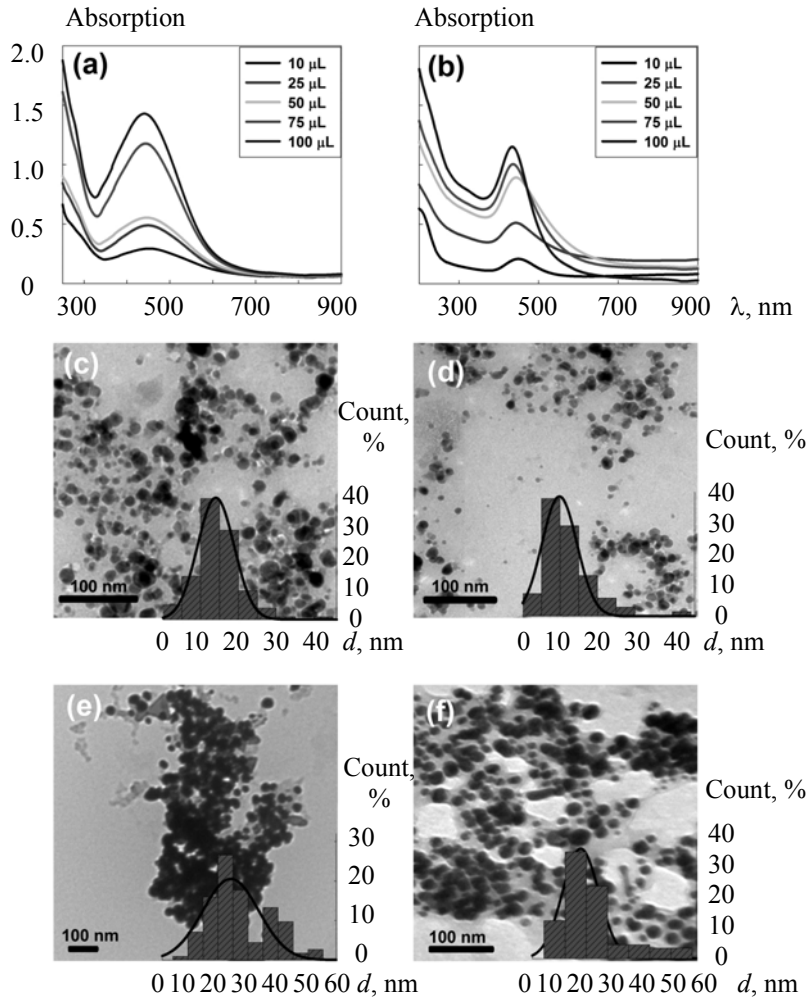

Fig. 1. UV-Vis spectra of (a) AgNPs and (b) AuNPs biosynthesized using different quantities of *F. sycomorus* extract. TEM images and their corresponding histograms (inset) of AgNPs prepared by the reaction of $AgNO_3$ (1 mM) with (c) 25 μL and (d) 100 μL of *F. sycomorus* extract. TEM images and their corresponding histograms (inset) of AuNPs prepared by the reaction of $HAuCl_4$ (0.5 mM) with (e) 25 μL and (f) 100 μL of *F. sycomorus* extract.

gy were formed. The particles became more separated from each other, with an average size of 18 nm. It is postulated that at low extract concentrations the produced NPs might not be stabilized effectively. In this case, free Au^{3+} ions are present in the reaction media at a large excess. As a result, these Au^{3+} ions might undergo diffusion on the surface of AuNPs, which is formed by primary growth. Thus, uncontrolled secondary growth might occur, resulting in increased particle size and probably the formation of some anisotropic AuNPs [8]. Given the above results, 100 μL *F. sycomorus* extract was determined to be the optimum extract quantity.

Effect of silver and gold ion concentrations. Figures 2a and b show the UV-vis spectra of AgNPs and AuNPs biosynthesized at different metal ion concentrations. The peak intensity of AgNPs increased, and a significant red-shift occurred as the $AgNO_3$ concentration increased (Fig. 2a). The gradual strengthening of the peak intensity represented an increase in the AgNPs concentration. However, the red-shifted SPR position might be due to the growth or aggregation/agglomeration of AgNPs caused by the reduced capping effect of *F. sycomorus* extract at higher metal ion concentrations [23]. The TEM image of AgNPs biosynthesized at 0.5 mM $AgNO_3$ is displayed in Fig. 2c. The particles have a semi-spherical shape with an average size of 8 nm, and no aggregation/agglomeration can be observed in this image unlike in the sample prepared with 1 mM $AgNO_3$ solution and 100 μL extract (Fig. 1d). Hence, 0.5 mM was considered the concentration

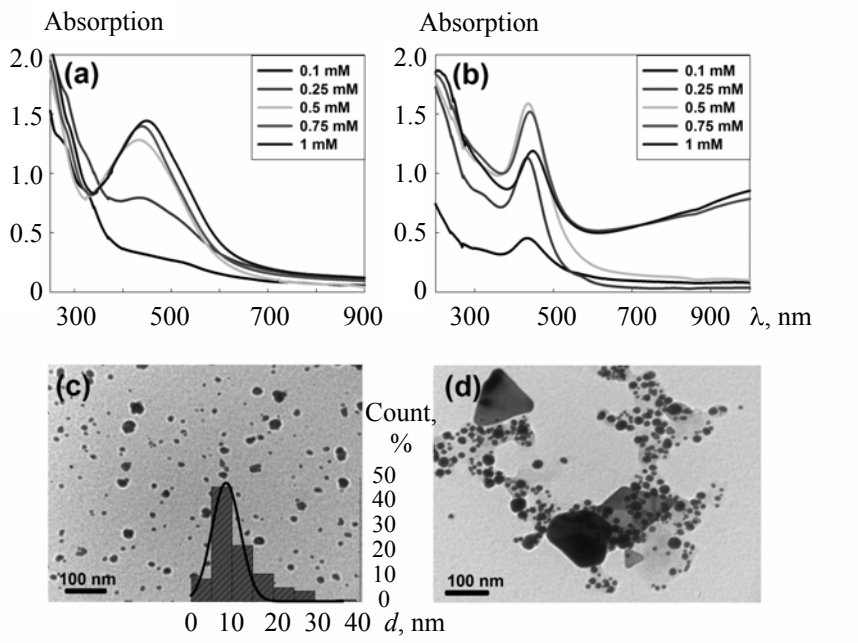

Fig. 2. UV-Vis spectra of (a) AgNPs and (b) AuNPs biosynthesized by the reaction of 100 μL of *F. sycomorus* extract with different metal ion concentrations. TEM images and their corresponding histograms (inset) of (c) AgNPs prepared at [$AgNO_3$] = 0.5 mM and (d) AuNPs prepared at [$HAuCl_4$] = 1 mM.

of $AgNO_3$ at which small AgNPs with no aggregation/agglomeration were produced. Aadil et al. [24] stated that the $AgNO_3$ concentration should be 0.5–1.0 mM to obtain small AgNPs. On the other hand, as the concentration of Au^{3+} ions increased from 0.1 to 0.5 mM, the SPR peak intensity of AuNPs showed an increasing trend with no remarkable shift in the wavelength (Fig. 2b). This indicated that increasing the concentration of Au^{3+} ions from 0.1 to 0.5 mM enhanced the reduction of Au^{3+} ions but did not considerably influence the particle size of AuNPs. A further increase in the Au^{3+} ion concentration from 0.5 to 1 mM reduced the band intensity and shifted the transverse SPR band to the lower energy side (from 534 to 545 nm). This observation indicated that AuNPs with larger sizes are formed at high metal ion concentrations. The UV-Vis spectra of AuNPs synthesized using both 0.75 and 1 mM Au^{3+} ions clearly showed a broad additional near-IR absorption band caused by excitation of the longitudinal (in-plane vibration) component of the SPR, which may indicate the formation of anisotropic AuNPs [25]. The TEM image of AuNPs prepared at 1 mM $HAuCl_4$ solution (Fig. 2d) indicated the formation of a mixture of spherical, triangular, and polygonal AuNPs. The sizes of the spherical AuNPs were around 5–20 nm. However, the anisotropic particles included large (120–160 nm) and small (18–45 nm) particles. Hence, the 0.5 mM $HAuCl_4$ concentration was chosen in terms of the high potential and definite shape of the NPs.

Effect of pH value. The UV-Vis spectra of AgNPs prepared at different pH values are shown in Fig. 3a. A very weak, broad SPR peak of AgNPs was observed at pH 1–4. This suppression of AgNPs formation may be due to the inactivation of the plant biomolecules under extremely acidic conditions [26]. Thereafter, within the pH range of 6–9, both the intensity and sharpness of the absorption maximum increased with a blue-shift, indicating an increase in the formation of small AgNPs with a narrow size distribution. In contrast, at pH 10 and 11, the peak intensity and sharpness decreased along with a red-shift, i.e. a smaller amount of larger AgNPs with wide size distribution were formed at very high pH values. A similar trend was observed by Khalil et al. [27] and Krishnaraj et al. [28]. Alkaline conditions are more favorable for the production of AgNPs. The presence of OH^- ions facilitates the ionization of functional groups (such as phenolic groups) in the extract, thereby allowing fast electron transfer to Ag^+ ions and reducing them to Ag^0. However, at very high pH values, the production of Ag_2O may be favorable and aggregation/agglomeration of NPs may occur [4]. Figure 3c represents the TEM image and histograms of AgNPs synthesized at pH 9. AgNPs became rather homogeneous in size and shape. The particles had a regular spherical shape with narrow size distribution and an average size of 4 nm. AgNPs were fully separated from each other and free from any aggregates. Therefore, pH 9 was favorable for the synthesis of monodispersed small spherical AgNPs using

F. sycomorus extract. Amin et al. synthesized small, highly dispersed AgNPs at pH 9 using *Solanum xanthocarpum* berry extract [9]. Figure 3b shows the UV–vis spectra of AuNPs prepared at different pH values. The intensity and sharpness of the AuNPs peak increased with a blue-shift as the pH value varied from 1 to 7, which implies that a high yield of small AuNPs with a narrow size distribution was obtained at pH 7. A further increase in the pH value resulted in a broadening, intensity decrease, and red shift of the SPR peak (at pH 9) before its decay at pH 10 and 11. Two SPR peaks for AuNPs were observed at both pH 3 and 4. This spectral change suggests the formation of another shape in addition to the spherical one, which was further confirmed by the TEM study. The TEM image of AuNPs prepared at pH 4 (Fig. 3d) suggested that the particles had a wide range of shapes and sizes. Triangular (34–215 nm) and hexagonal (42–216 nm) nanoplates were observed in addition to the spherical AuNPs (8–28 nm). At pH 7 (Fig. 3e), the obtained AuNPs were mainly spherical (11 nm), which was in agreement with the single SPR peak that appeared in the UV-Vis results (Fig. 3b). The particles were well separated and free from aggregates/agglomerates. These findings accord well with previously reported data [3, 29]. Therefore, pH 7 was the most favorable pH value for the synthesis of monodispersed small AuNPs with a definite shape using *F. sycomorus* extract. The effect of the pH value on the synthesis of AuNPs can be explained by considering the pH-dependent hydrolysis of chloroauric acid. With increasing pH, $AuCl_4^-$ ions give rise to $[AuCl_{4-n}(OH)_n]^-$ complex ions through a stepwise substitution of Cl^- ligands by OH^-. The speciation of $HAuCl_4$ had a great effect on the synthesis, structure, and properties of AuNPs [5].

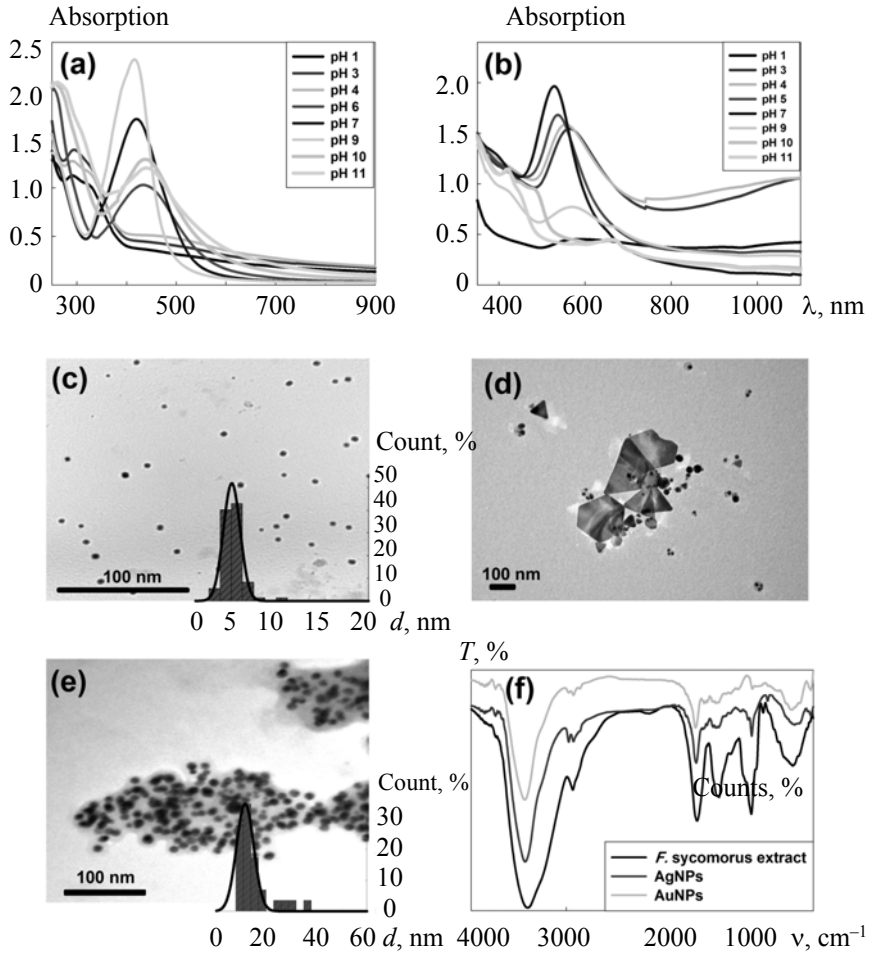

Fig. 3. UV-Vis spectra of (a) AgNPs and (b) AuNPs biosynthesized by the reaction of 100 μL of *F. sycomorus* extract with 0.5 mM of $AgNO_3$ or $HAuCl_4$ at different pH values. TEM images and their corresponding histograms (inset) of (c) AgNPs prepared at pH 9, (d) AuNPs prepared at pH 4, and (e) AuNPs prepared at pH 7. (f) FT-IR spectra of 70% *F. sycomorus* methanolic extract, AgNPs and AuNPs stabilized by the extract.

FTIR spectroscopic data. FTIR spectroscopic studies were carried out to investigate the potential biomolecules in *F. sycomorus* leaf extract responsible for the reduction and capping of the bioreduced AgNPs and AuNPs. The IR spectrum of the leaf extract (Fig. 3f) showed a strong broad peak at 3405 cm^{-1}. This peak was referred to as the stretching vibrations of the O–H groups attributed to the alcoholic and phenolic groups [30]. This band became sharper and shifted to 3430 and 3437 cm^{-1} upon the reactions with the Ag^{+} and Au^{3+} ions, respectively. The O–H bending vibration band was observed at 1621 cm^{-1}, with contribution from aromatic C=C stretching vibrations [11]. This band shifted to a high wavenumber after the formation of the AgNPs and AuNPs. The spectral range from 1500 to 1200 cm^{-1} showed remarkable structural changes. The leaf extract spectrum displayed two peaks (at 1400 and 1265 cm^{-1}). The band centered at 1400 cm^{-1} represented the stretching vibration of aromatic compounds and bending vibrations of C–H groups. However, the small peak that appeared as a shoulder at 1265 cm^{-1} was assigned as the stretching vibrations of C_{arom}–O groups [31]. These two peaks were deformed and split into several very weak bands in the AgNPs and AuNPs samples. Moreover, the region between 1200 and 950 cm^{-1} showed a structured signal centered at 1052 cm^{-1}, which was due to overlap between the C–H molecular vibrations of sugar moieties and the C–OH (stretching) of pyran-derived compounds (such as flavonoids, condensed tannins, and sugars) [11]. This peak became very weak in the AgNPs and nearly disappeared in the AuNPs. These spectral changes in the hydroxyl, aryl, and ether groups suggested that phenolic compounds and/or glycosides may play a critical role in NPs capping.

Active biomolecules in 70% methanolic F. sycomorus extract. Generally, the curative properties of the *Ficus* species can be attributed to the presence of phenolic compounds. Abdel-Hameed [16] revealed that the major components of the methanolic extract of *F. sycomorus* leaves are phenolic compounds, which are mainly flavonoids and tannins. The active biomolecules responsible for the antioxidant activity of the 70% methanolic extract of *F. sycomorus* leaves were isolated and identified as flavonoid glycosides derived from quercetin (including isoquercitrin, rutin, quercetin-3,7-*O*-α-L-dirhamnoside, and quercetin-3-*O*-β-D-galactopyranosyl(1→6)glucopyranoside) in addition to the flavonoid aglycon quercetin [32]. Thus, the presence of these phytochemicals in *F. sycomorus* leaf extract might account for its potential for bioreduction of metal ions. These results were consistent with our FTIR results and literature data. Many researchers have reported the biosynthesis of metal NPs using flavonoids and their glycosides [33–36].

Catalytic activity of AgNPs and AuNPs. The chemocatalytic activity of the biosynthesized NPs on the reduction of MB by $NaBH_4$ was evaluated in an aqueous solution. The kinetics of the catalytic reduction was investigated by measuring the residual concentration of the dye at different time intervals using a spectrophotometer. Figure 4a shows the UV-Vis spectra of the MB solution without the nanocatalyst after reduction by $NaBH_4$ for 90 min. MB showed a strong maximum absorption wavelength at λ_{max} = 665 nm due to π–π* electronic transitions with an absorption shoulder at 615 nm [37]. The spectra exhibited no considerable decrease in the absorption peak, indicating the poor MB reduction rate in the absence of a catalyst. Upon addition of the catalyst into the reaction medium, the characteristic blue color of MB disappeared after some time, indicating the complete reduction of the dye. This observation was monitored by recording the UV-Vis spectra during the reduction course (Figs. 4b and c). As seen in the figures, the intensity of the absorption peak decreased markedly, indicating the reduction of MB by $NaBH_4$ in the presence of the nanocatalyst. The reaction was completed within 12 and 18 min in the presence of AgNPs and AuNPs, respectively. Hence, the degradation of MB dye was enhanced significantly after the addition of AgNPs and AuNPs as catalysts. The reduction process occurred via the adsorption of reactants on the nanocatalyst surface, which had an ample surface area. Subsequent redox reactions happened through an electron transfer reaction where BH_4^- ions are the electron reservoirs and the MB dye molecules are the acceptors, resulting in the degradation of the dye [38, 39]. In the reaction mixture, since $NaBH_4$ was used in a higher excess concentration than that of MB, the reduction rate was assumed to be independent of the $NaBH_4$ concentration. The degradation of MB was considered to follow pseudo-first order kinetics, and this process is expressed by the following one-dimensional kinetic equation:

$$\ln(C_t/C_0) = \ln(A_t/A_0) = -k_{app},$$

where C_0 and C_t are the MB concentrations at the beginning and at any time t, respectively, A_0 and A_t are their corresponding absorbances at 665 nm, and k_{app} is the kinetic constant. The plot of $\ln(A_t/A_0)$ versus time (Fig. 4d) generated a straight line, from which the k_{app} values of the catalytic reactions were calculated as the slope of the plot. The rate of MB degradation (k_{app} = 0.156 min^{-1}) in a solution containing AgNPs was higher than that of AuNPs (k_{app} = 0.094 min^{-1}). Table 1 shows the reported k_{app} of MB catalytic reduction using the

plant-biosynthesized AgNPs and AuNPs. The k_{app} values in the present study are comparable with those from previous works.

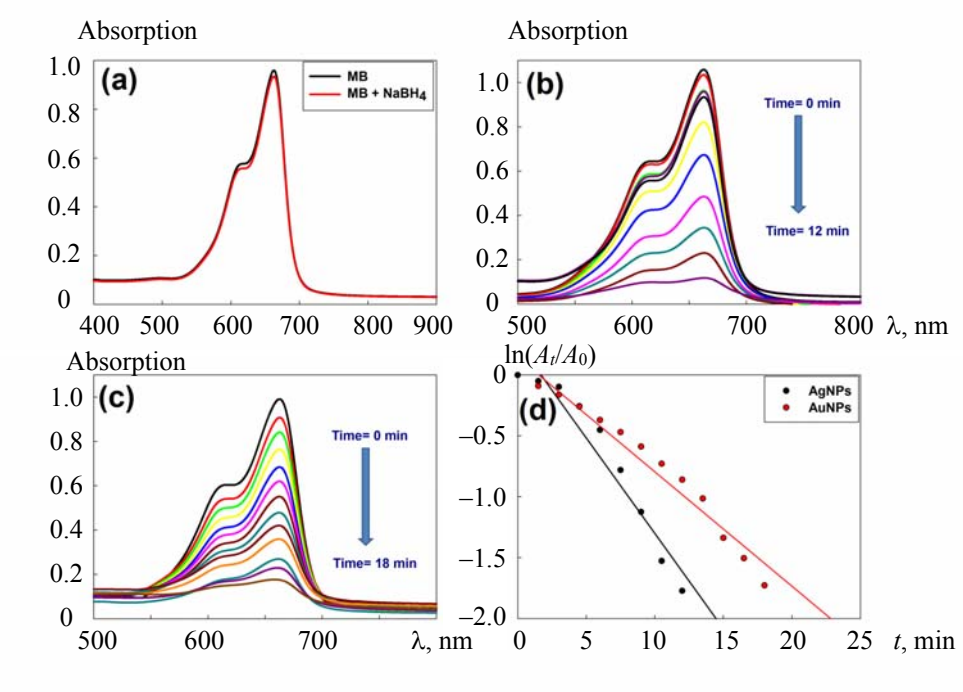

Fig. 4. (a) UV-Vis spectra of MB before and after addition of $NaBH_4$. Time-dependent UV-Vis spectra of MB reduction in the presence of (b) AgNP and (c) AuNPs. (d) $\ln(A_t/A_0)$ versus reaction time.

TABLE 1. The Catalytic Reduction of MB Over Different Phytosynthesized AgNPs and AuNPs Catalysts

Catalyst	k_{app}, min^{-1}	Reference
Kalanchoe Daigremontiana/Ag	1.879	[40]
Albizia procera/Ag	0.0051	[41]
Lantana camara/Ag	0.0034	[42]
Morinda citrifolia/Ag	0.032	[43]
Terminalia bellerica/Ag	0.029	[44]
Areca catechu nut/Ag	0.3415	[45]
Guggulutiktham Kashayam/Ag	0.224	[46]
Mentha aquatica/Ag	0.126	[47]
Diospyros lotus/Ag	0.121	[48]
F. sycamorus/Ag	0.156	This work
Morinda citrifolia/Au	0.432	[43]
Lagerstroemia speciosa/Au	0.264	[49]
Sesbania grandiflora/Au	0.041	[50]
Sterculia acuminate/Au	0.043	[51]
Plukenetia volubilis/Au	0.003	[52]
Momordica cochinchinensis/Au	0.296	[53]
Parkia roxburghii/Au	0.263	[54]
F. sycamorus/Au	0.094	This work

Conclusions. A straightforward, green route has been reported for the synthesis of AgNPs and AuNPs using *F. sycomorus* leaf extract as a cost-effective, renewable reducing and capping agent. The optimal conditions for producing monodispersed small NPs of definite shapes were detected as follows: (a) for AgNPs, 100 µL extract/5 mL of 0.5 mM $AgNO_3$ solution at pH 9, and (b) for AuNPs, 100 µL extract/5 mL of 0.5 mM $HAuCl_4$ solution at pH 7. Sugars and phenolics (mainly flavonoid glycosides) were the main constituents in *F. sycomorus* leaf extract that play a major role in NPs reduction and stabilization. *F. sycomorus*-stabilized NPs showed good catalytic activity in MB reduction. The catalytic rate constant for AgNPs (0.156 min^{-1}) was higher than that of AuNPs (0.094 min^{-1}).

REFERENCES

1. A. V. Kalenskii, A. A. Zvekov, A. P. Nikitin, *J. Appl. Spectrosc.*, **83**, 1020–1025 (2017).
2. P. Slepička, N. Slepičková Kasálková, J. Siegel, Z. Kolská, V. Švorčík, *Materials*, **13**, 1 (2019).
3. S. He, Z. Guo, Y. Zhang, S. Zhang, J. Wang, N. Gu, *Mater. Lett*., **61**, 3984–3987 (2007).
4. A. Zuorro, A. Iannone, S. Natali, R. Lavecchia, *Processes*, **7**, 193 (2019).
5. S. Wang, K. Qian, X. Bi, W. Huang, *J. Phys. Chem. C*, **113**, 6505–6510 (2009).
6. M. F. Zayed, W. H. Eisa, S. M. El-Kousy, W. K. Mleha, N. Kamal, *Spectrochim. Acta A, Mol. Biomol. Spectrosc.*, **214**, 496–512 (2019).
7. Y. Foo, V. Periasamy, L. Kiew, G. Kumar, S. Malek, *Nanomaterials,* **7**, 123 (2017).
8. S. Phukan, P. Bharali, A. K. Das, M. H. Rashid, *RSC Adv*., **6**, 49307–49316 (2016).
9. M. Amin, F. Anwar, M. R. S. A. Janjua, M. A. Iqbal, U. Rashid, *Int. J. Mol. Sci*., **13**, 9923–9941 (2012).
10. S. Iravani, *Green Chem*., **13**, 2638 (2011).
11. M. F. Zayed, R. A. Mahfoze, S. M. El-kousy, E. A. Al-Ashkar, *Colloids Surf. A: Physicochem. Eng. Aspects,* **585**, 124167 (2020).
12. C. Shi, N. Zhu, Y. Cao, P. Wu, *Nanoscale Res. Lett.*, **10** (2015).
13. N. Konai, D. Raidandi, A. Pizzi, L. Meva'a, *Eur. J. Wood and Wood Prod*., **75**, 807–815 (2017).
14. O. Mousa, P. Vuorela, J. Kiviranta, S. A. Wahab, R. Hiltunen, H. Vuorela, *J. Ethnopharmacol.*, **41**, 71–76 (1994).
15. H. S. Foyet, S. Tchinda Deffo, P. Koagne Yewo, I. Antioch, S. Zingue, E. A. Asongalem, P. Kamtchouing, A. Ciobica, *BMC Complementary Altern. Med.*, **17** (2017).
16. E.-S. S. Abdel-Hameed, *Food Chem.*, **114**, 1271–1277 (2009).
17. M. Amjadi, T. Sodouri, *J. Appl. Spectrosc.*, **81**, 232–237 (2014).
18. R. A. Boitor, I. S. Tódor, L. F. Leopold, N. Leopold, *J. Appl. Spectrosc.*, **82**, 415–419 (2015).
19. N. Esmaile, M. R. Sohrabi, F. Motiee, *J. Appl. Spectrosc.*, **87**, 372–377 (2020).
20. R. R. Shamilov, V. I. Nuzhdin, V. F. Valeev, Y. G. Galyametdinov, A. L. Stepanov, *J. Appl. Spectrosc.*, **82**, 773–778 (2015).
21. E. Seo, S.-J. Ko, S. H. Min, J. Y. Kim, B.-S. Kim, *Chem. Mater*., **27**, 4789–4798 (2015).
22. A. D. Dwivedi, K. Gopal, *Colloids Surf. A: Physicochem. Eng. Aspects*, **369**, 27–33 (2010).
23. P. Galinetto, A. Taglietti, L. Pasotti, P. Pallavicini, G. Dacarro, E. Giulotto, M. S. Grandi, *J. Appl. Spectrosc.,* **82**, 1052–1059 (2016).
24. K. R. Aadil, A. Barapatre, A. S. Meena, H. Jha, *Int. J. Biol. Macromol.*, **82**, 39–47 (2016).
25. M. F. Zayed, W. H. Eisa, A. M. Hezma, *J. Appl. Spectrosc.*, **83**, 1046–1050 (2017).
26. N. Yang, W.-H. Li, *Ind. Crops Prod.*, **48**, 81–88 (2013).
27. M. M. H. Khalil, E. H. Ismail, K. Z. El-Baghdady, D. Mohamed, *Arab. J. Chem*., **7**, 1131–1139 (2014).
28. C. Krishnaraj, R. Ramachandran, K. Mohan, P. T. Kalaichelvan, *Spectrochim. Acta A: Mol. Biomol. Spectrosc.,* **93**, 95–99 (2012).
29. Y. Li, Y. Li, Q. Li, X. Fan, J. Gao, Y. Luo, *J. Chem*., **2016**, 1–7 (2016).
30. M. F. Zayed, W. H. Eisa, *Spectrochim. Acta A: Mol. Biomol. Spectrosc*., **121**, 238–244 (2014).
31. G. Tondi, A. Petutschnigg, *Ind. Crops Prod.*, **65**, 422–428 (2015).
32. M. M. M. El-Sayed, M. A.-A. El-Nahas, H. A.-K. El-Sayed, W. El-Eman, Ghareeb Mosad, *Pharmacologyonline*, **3**, 317–332 (2010).
33. F. Tasca, R. Antiochia, *Nanomaterials*, **10**, 909 (2020).
34. M. S. Coutinho, E. Latocheski, J. M. Neri, A. C. O. Neves, J. B. Domingos, L. N. Cavalcanti, L. H. S. Gasparotto, E. P. Moraes, F. G. Menezes, *RSC Adv.*, **9**, 30007–30011 (2019).
35. Z. D. Ozdal, E. Sahmetlioglu, I. Narin, A. Cumaoglu, *Biotech*., **9** (2019).

36. N. Sahu, D. Soni, B. Chandrashekhar, D. B. Satpute, S. Saravanadevi, B. K. Sarangi, R. A. Pandey, *Int. Nano Lett.*, **6**, 173–181 (2016).
37. A. M. Atta, Y. M. Moustafa, H. A. Al-Lohedan, A. O. Ezzat, A. I. Hashem, *ACS Omega*, **5**, 2829–2842 (2020).
38. N. G. Bastús, F. Merkoçi, J. Piella, V. Puntes, *Chem. Mater.*, **26**, 2836–2846 (2014).
39. A. Bhargava, N. Jain, M. A. Khan, V. Pareek, R. V. Dilip, J. Panwar, *J. Environ. Manag*., **183**, 22–32 (2016).
40. G. A. Molina, R. Esparza, J. L. López-Miranda, A. R. Hernández-Martínez, B. L. España-Sánchez, E. A. Elizalde-Peña, M. Estevez, *Colloids Surf. B: Biointerfaces*, **180**, 141–149 (2019).
41. M. Rafique, I. Sadaf, M. B. Tahir, M. S. Rafique, G. Nabi, T. Iqbal, K. Sughra, *Mater. Sci. Eng. C*, **99**, 1313–1324 (2019).
42. B. Kumar, K. Smita, L. Cumbal, *J. Sol-Gel Sci. Technol.,* **78**, 285–292 (2015).
43. S. Francis, K. M. Nair, N. Paul, E. P. Koshy, B. Mathew, *Mater. Today: Proc*., **9**, 97–104 (2019).
44. L. Sherin, A. Sohail, U.-e.-S. Amjad, M. Mustafa, R. Jabeen, A. Ul-Hamid, *Colloid Interface Sci. Commun.*, **37**, 100276 (2020).
45. A. Rajan, V. Vilas, D. Philip, *J. Mol. Liquids,* **207**, 231–236 (2015).
46. V. S. Suvith, D. Philip, *Spectrochim. Acta A: Mol. Biomol. Spectrosc.*, **118**, 526–532 (2014).
47. A. Nouri, M. Tavakkoli Yaraki, A. Lajevardi, Z. Rezaei, M. Ghorbanpour, M. Tanzifi, *Colloid Interface Sci. Commun.*, **35**, 100252 (2020).
48. S. Hamedi, S. A. Shojaosadati, *Polyhedron*, **171**, 172–180 (2019).
49. B. C. Choudhary, D. Paul, T. Gupta, S. R. Tetgure, V. J. Garole, A. U. Borse, D. J. Garole, *J. Environ. Sci*., **55**, 236–246 (2017).
50. J. Das, P. Velusamy, *J. Taiwan Inst. Chem. Eng*., **45**, 2280–2285 (2014).
51. N. K. R. Bogireddy, K. K. Hoskote Anand, B. K. Mandal, *J. Mol. Liq*., **211**, 868–875 (2015).
52. B. Kumar, K. Smita, L. Cumbal, A. Debut, *J. Photochem. Photobiol. B: Biol.*, **158**, 55–60 (2016).
53. B. Paul, B. Bhuyan, D. D. Purkayastha, S. Vadivel, S. S. Dhar, *Mater. Lett.,* **185**, 143–147 (2016).
54. B. Paul, B. Bhuyan, D. D. Purkayastha, S. S. Dhar, *J. Photochem. Photobiol. B: Biol*., **154**, 1–7 (2016).